The Journal of Chemical Physics

Impact of the current density on paramagnetic NMR properties EP

Cite as: J. Chem. Phys. **157**, 031102 (2022); https://doi.org/10.1063/5.0103898
Submitted: 17 June 2022 • Accepted: 24 June 2022 • Accepted Manuscript Online: 27 June 2022 •
Published Online: 15 July 2022

Yannick J. Franzke and Christof Holzer

AIP Publishing

The Journal of Chemical Physics COMMUNICATION scitation.org/journal/jcp

Impact of the current density on paramagnetic NMR properties

Cite as: J. Chem. Phys. 157, 031102 (2022); doi: 10.1063/5.0103898
Submitted: 17 June 2022 • Accepted: 24 June 2022 •
Published Online: 15 July 2022

Yannick J. Franzke[1,a)] and **Christof Holzer**[2,a)]

AFFILIATIONS

[1] Fachbereich Chemie, Philipps-Universität Marburg, Hans-Meerwein-Straße 4, 35032 Marburg, Germany
[2] Institute of Theoretical Solid State Physics, Karlsruhe Institute of Technology (KIT), Wolfgang-Gaede-Straße 1, 76131 Karlsruhe, Germany

[a)] **Authors to whom correspondence should be addressed:** yannick.franzke@chemie.uni-marburg.de and christof.holzer@kit.edu

ABSTRACT

Meta-generalized gradient approximations (meta-GGAs) and local hybrid functionals generally depend on the kinetic energy density τ. For magnetic properties, this necessitates generalizations to ensure gauge invariance. In most implementations, τ is generalized by incorporating the external magnetic field. However, this introduces artifacts in the response of the density matrix and does not satisfy the iso-orbital constraint. Here, we extend previous approaches based on the current density to paramagnetic nuclear magnetic resonance (NMR) shieldings and electron paramagnetic resonance (EPR) g-tensors. The impact is assessed for main-group compounds and transition-metal complexes considering 25 density functional approximations. It is shown that the current density leads to substantial improvements—especially for the popular Minnesota and strongly constrained and appropriately normed (SCAN) functional families. Thus, we strongly recommend to use the current density generalized τ in paramagnetic NMR and EPR calculations with meta-GGAs.

I. INTRODUCTION

Meta-generalized gradient approximations (meta-GGAs) are formally the most accurate approach in semilocal density functional theory (DFT).[1,2] The key ingredient is the kinetic energy density τ. Magnetic properties, such as nuclear magnetic resonance (NMR) shielding constants and coupling constants, are formulated by generalizing the kinetic energy with the vector potential of the magnetic interaction. In turn, this means that τ also needs to be generalized to ensure consistency and a proper physical behavior, including gauge invariance.[3–10] The most straightforward ansatz is to include the vector potential of the external magnetic field $\vec{B}$ into τ.[3] However, this violates the iso-orbital constraint and is impractical for the vector potential of magnetic moments, which is employed to compute NMR spin–spin coupling constants and hyperfine coupling constants in electron paramagnetic resonance (EPR) spectroscopy. A generalization based on the (paramagnetic) current density according to Dobson[4,5,11] is a more suitable ansatz.[12–14] Matters are similar for excitation energies[7,15] and other electromagnetic properties. Furthermore, the current density functional framework is also the method of choice in finite field approaches.[16–21]

It was shown recently that the current density is also advantageous for NMR shifts of closed-shell molecules in the limit of a vanishing magnetic field.[22] The current-dependent generalization not only improves the results in practical NMR shift calculations[23] but also removes artifacts in the response of the density matrix.[22] For instance, the term involving the linear response of the density strictly vanishes for closed-shell atoms.[22] Moreover, the iso-orbital constraint is restored, which is of great importance for meta-GGAs and local hybrid functionals (LHFs).[24,25] The latter allow for a position-dependent admixture of exact exchange based on the iso-orbital indicator,[24] the correlation length,[26] or more involved approximations.[27]

Herein, we extend the current-dependent generalization of τ to open-shell systems and paramagnetic NMR shielding constants and the related g-tensor in EPR spectroscopy. This allows us to consider all NMR and EPR properties of open- and closed-shell systems on an equal footing.

II. THEORY

NMR shielding constants and g-tensors depend on the derivative of the density matrix D with respect to the magnetic field $\vec{B}$,[28–31] which is introduced by the minimal coupling and the vector potential,

$$\vec{A}_O(\vec{r}) = \frac{1}{2}\vec{B} \times \vec{r}_O. \tag{1}$$

This introduces a dependence on the gauge origin O. Yet, all physical properties need to be independent of O. To ensure gauge-origin invariance, the kinetic energy density

$$\tau_\sigma = \sum_j \nabla\varphi_{j,\sigma}^* \nabla\varphi_{j,\sigma} \tag{2}$$

of the Kohn–Sham spin orbitals φ_σ may be generalized as[3]

$$\tilde{\tau}_{\mathrm{MS},\sigma} = \tau_\sigma + \frac{1}{c}\vec{j}_{p,\sigma} \cdot \vec{A}_O + \frac{1}{2c^2}\left|\vec{A}_O\right|^2 \rho_\sigma, \tag{3}$$

with the particle density ρ and the paramagnetic current density[32]

$$\vec{j}_{p,\sigma} = -\frac{\mathrm{i}}{2}\sum_j\left(\varphi_{j,\sigma}^*\vec{\nabla}\varphi_{j,\sigma} - \varphi_{j,\sigma}\vec{\nabla}\varphi_{j,\sigma}^*\right). \tag{4}$$

This allows for a straightforward differentiation with respect to the magnetic field in order to compute the first-order perturbed Kohn–Sham–Fock matrix using

$$\left[\frac{\partial\tilde{\tau}_{\mathrm{MS},\sigma}}{\partial D_{\mu\nu,\sigma}}\right]^{B_u} = \left[\frac{1}{2}\nabla\chi_\mu^*\nabla\chi_\nu + \frac{\mathrm{i}}{2}\vec{A}_O\left(\chi_\nu\nabla\chi_\mu^* - \chi_\mu^*\nabla\chi_\nu\right)\right]^{B_u}, \tag{5}$$

where the superscript B_u denotes the derivative with respect to the component u of the field and χ are gauge-including atomic orbitals.[33,34] Note that the derivative is formed in the limit of a vanishing perturbation.

A more rigorous generalization[4,5,11] is solely based on $\vec{j}_p$ with

$$\tilde{\tau}_{\mathrm{D},\sigma} = \tau_\sigma - \frac{\vec{j}_{p,\sigma}^{\,2}}{2\rho_\sigma}. \tag{6}$$

This is a more universal approach as the current density does not depend explicitly on the vector potential, i.e., the dependence arises due to field-dependent basis functions and the density matrix.[22] Herein, we neglect the current density in the ground-state calculation, i.e., $\vec{j}_p$ vanishes in the limit $\vec{B} \to 0$. The magnetic-field derivative becomes

$$\left[\frac{\partial\tilde{\tau}_{\mathrm{D},\sigma}}{\partial D_{\mu\nu,\sigma}}\right]^{B_u} = \left[\frac{1}{2}\nabla\chi_\mu^*\nabla\chi_\nu + \frac{\mathrm{i}}{2\rho_\sigma}\vec{j}_{p,\sigma}\left(\chi_\nu\nabla\chi_\mu^* - \chi_\mu^*\nabla\chi_\nu\right)\right]^{B_u}, \tag{7}$$

where both Eqs. (5) and (7) are evaluated numerically on a grid. For $\tilde{\tau}_{\mathrm{D}}$, this always requires an iterative procedure for the derivative of $\vec{j}_{p,\sigma}$, while a one-shot procedure can be used for pure functionals with $\tilde{\tau}_{\mathrm{MS}}$. Note that the response of the density matrix D^{B_u} is also used to compute magnetically induced current densities or ring currents,[35–42] as well as magnetizabilities.[9] Equation (7) holds for non- or scalar-relativistic ground-states. It does not hold when considering spin–orbit coupling self-consistently or when considering explicit non-vanishing magnetic fields.

III. COMPUTATIONAL DETAILS

The outlined approach was implemented into TURBOMOLE.[43–45] The implementation of local hybrid functionals[12,46,47] was extended to the unrestricted Kohn–Sham framework by forming the spin-up and spin-down quantities, e.g., $\rho_\uparrow = \rho + s$ and $\rho_\downarrow = \rho - s$ with the total density ρ and the spin density s. LHFs use a seminumerical scheme for a simultaneous evaluation of the semilocal DFT and exact exchange.[48–50]

First, we assess the importance for non-relativistic pNMR shieldings of small main-group molecules with the aug-cc-pVTZus5t[51–54] and the def2-TZVPP basis sets.[55] Second, g-tensors of 4d complexes are studied with the local exact two-component (DLU-X2C) Hamiltonian[56–61] and the x2c-QZVPall-2c basis set;[62] spin–orbit coupling is treated perturbatively.[14] Third, magnetically induced current densities of $[\mathrm{UBi}_{12}]^{3-}$, prepared in Ref. 63, are computed with the GIMIC code[36–41] and the def(2)-TZVP basis,[55,64–66] making use of the resolution of the identity approximation.[67]

Throughout this work, we consider 25 density functional approximations, namely, TPSS,[68] TPSSh,[68,69] r^{2}SCAN,[70,71] r^{2}SCANh,[70–72] r^{2}SCAN0,[70–72] r^{2}SCAN50,[70–72] Tao–Mo,[73] M06-L,[74] M06,[75] M06-2X,[75] M11-L,[76] M11,[77] MN12-L,[78] MN12-SX,[79] MN15-L,[80] MN15,[81] PKZB,[82] BMK,[83] B97M,[84] ωB97M,[85] TASK,[86] LH12ct-SsirPW92 (LH12ct),[87] LH20t,[88] LHJ14,[26] and mPSTS-a1.[12,27] We refer to the supplementary material for the complete computational settings and the individual results for the statistical evaluation.

IV. RESULTS

A. Impact on pNMR shielding constants

The NMR shielding constants of BH_2, CH_2^-, NH_2, $\mathrm{C}_4\mathrm{H}_4$ (triplet), B_3, and Al_3 are listed in Table I. The largest changes are observed for the M06 family. The field-dependent generalization leads to notable deviations toward the restricted active space self-consistent field (RASSCF)coupled-cluster singles and doubles (CCSD) results, whereas the results with the current-dependent $\tilde{\tau}_{\mathrm{D}}$ are in rather good agreement. Especially for BH_2, drastic changes of more than 100% are found with M06-2X. In contrast, smaller shifts from $\tilde{\tau}_{\mathrm{MS}}$ to $\tilde{\tau}_{\mathrm{D}}$ are present for TPSS, TPSSh, and r^{2}SCAN. Yet, $\tilde{\tau}_{\mathrm{D}}$ also significantly improves the results for these functionals. The impact of $\tilde{\tau}_{\mathrm{D}}$ on pNMR shieldings is distinctly larger than for its closed-shell counterpart.[22] This hints at a more pronounced contribution of the nonphysical artifacts in the paramagnetic orbital part, which is the leading term for the heavy element shielding constants of BH_2, CH_2^-, and NH_2. The maximum change is observed for the zz component of the tensor when placing the molecule in the xy plane.

B. g-Tensors of transition-metal complexes

The dependence of the g-tensor on τ is shown in Fig. 1. Here, the percent-wise deviation of τ_{MS} and τ_{D} is shown for $[\mathrm{MoNCl}_4]^{2-}$, $[\mathrm{MoOF}_4]^-$, $[\mathrm{MoOCl}_4]^-$, $[\mathrm{MoOF}_5]^{2-}$, $[\mathrm{MoOBr}_5]^{2-}$, $[\mathrm{TcNF}_4]^-$, $[\mathrm{TcNCl}_4]^-$, and $[\mathrm{TcNBr}_4]^-$. The largest impact is observed for TASK with 43.4%; the latest Minnesota functionals MN15-L and MN15 rank second and third. For TASK, this can be rationalized as it has been designed to yield a steep change in the enhancement factor as a function of τ. The Minnesota functionals

TABLE I. Impact of the current-dependent generalization of τ on the isotropic orbital contribution to the pNMR shieldings with various density functional approximations and the aug-cc-pVTZus5t/def2-TZVPP basis set. Results with the field-dependent generalization by Maximoff and Scuseria serve as reference. Wave-function based results (RASSCF/aug-cc-pVTZus5t and CCSD/def2-TZVPP) are taken from Refs. 37 and 54. The nucleus of interest is given in parentheses. See the supplementary material for the results with all functionals.

Functional	BH$_2$ (B)	BH$_2$ (H)	CH$_2$ (C)	CH$_2^-$ (H)	NH$_2$ (B)	NH$_2$ (H)	C$_4$H$_4$ (C)	C$_4$H$_4$ (H)	B$_3$ (B)	Al$_3$ (Al)
TPSS	−77.95	15.20	26.31	24.62	−137.05	19.33	55.57	24.51	141.49	589.55
cTPSS	−98.26	13.89	16.52	24.15	−163.79	18.52	55.12	24.51	142.17	589.77
TPSSh	−83.81	14.69	23.91	24.41	−145.45	18.95	55.50	24.47	141.63	591.73
cTPSSh	−103.33	13.40	14.65	23.96	−170.94	18.17	55.10	24.46	142.24	591.82
r^{2}SCAN	−53.57	16.48	61.35	25.21	−70.56	20.19	64.09	24.21	142.42	607.66
cr^{2}SCAN	−89.02	13.88	42.22	24.72	−117.93	19.12	60.18	24.32	141.92	599.54
M06-L	−35.21	18.25	45.34	24.86	−80.75	20.30	58.06	24.52	137.91	598.13
cM06-L	−52.09	16.44	36.50	24.39	−115.90	19.10	55.27	24.46	138.62	596.79
M06	−244.39	2.81	−35.82	21.15	−277.27	14.36	37.12	24.24	131.09	556.88
cM06	−156.75	9.07	−9.55	22.10	−240.69	15.24	38.83	24.12	131.88	560.12
M06-2X	−901.58	−47.61	−147.98	15.02	−541.72	6.14	29.85	23.49	133.23	539.56
cM06-2X	−280.87	−0.03	−59.21	19.86	−343.62	12.58	35.41	23.56	134.20	553.39
RASSCF	−167.62	7.05	−19.38	19.69	−291.08	12.95	...	...	...	...
CCSD	...	...	...	...	...	...	61.06	24.32	141.8/140.7	606

also generally exhibit a large dependence on τ, and accordingly, the results benefit from the consideration of the paramagnetic current density. M06 is a notable exception in this regard with relative changes of about 5%. The strongly constrained and appropriately normed (SCAN) family represents an intermediate case with τ-dependent shifts between 16% and 9% [mean absolute percent-wise deviation (MAPD)]. Compared to TASK, indeed, a less steep dependence of the enhancement factor on τ is expected in SCAN. The admixture of exact exchange alleviates the impact of $\tilde{\tau}_{\mathrm{D}}$ in SCAN. A similar picture is revealed for TPSS and TPSSh with MAPDs of 7.0% and 4.7%. For the hybrid functionals BMK and ωB97M, $\tilde{\tau}_{\mathrm{D}}$ leads to almost no change, as the MAPDs are below 3%. This is in striking contrast to B97M with an MAPD of 21.2% and no inclusion of exact exchange.

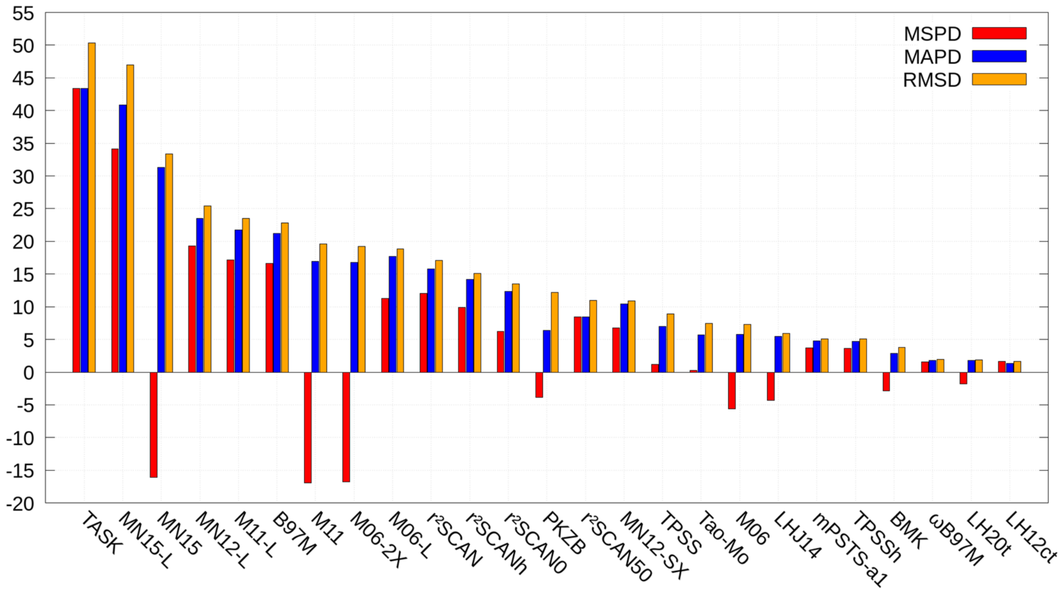

FIG. 1. Impact of the current-dependent generalization of τ for various density functional approximations on the isotropic Δg-shift of [MoNCl$_4$]$^{2-}$, [MoOF$_4$]$^-$, [MoOCl$_4$]$^-$, [MoOF$_5$]$^{2-}$, [MoOBr$_5$]$^{2-}$, [TcNF$_4$]$^-$, [TcNCl$_4$]$^-$, and [TcNBr$_4$]$^-$. Results with the field-dependent generalization by Maximoff and Scuseria serve as reference. We list the mean signed percent-wise deviation (MSPD), the mean absolute percent-wise deviation (MAPD), and the root mean square deviation (RMSD).

TABLE II. Ring current strength of $[\mathrm{UBi}_{12}]^{3-}$ in nA/T with various density functional approximations. All functionals predict a net diatropic ring current. See the supplementary material for the results with all functionals.

Functional	Ring current	Functional	Ring current
TPSS	17.3	M06-L	17.5
cTPSS	17.6	cM06-L	18.2
TPSSh	17.4	M06	18.9
cTPSSh	17.7	cM06	17.4
r^{2}SCAN	17.3	M06-2X	15.8
cr^{2}SCAN	17.9	M06-2X	14.8

The local hybrid functionals LH12ct, LH20t, LHJ14, and mPSTS-a1 show no pronounced dependence on the current density. This is in line with the observation that exact exchange reduces the impact of $\tilde{\tau}_{\mathrm{D}}$. Here, the main benefit of this generalization is the fulfillment of the iso-orbital constraint for the local mixing function in LH12ct and LH20t.

C. Ring current of $[\mathrm{UBi}_{12}]^{3-}$

The cluster $[\mathrm{UBi}_{12}]^{3-}$ consists of a U^{4+} core and a Bi_{12}^{7-} radical shell,[63] which sustains a strong diatropic (aromatic) ring current.[12,60,89] The ring current strengths of $[\mathrm{UBi}_{12}]^{3-}$ are listed in Table II. Here, the generalization of τ may change the results by up to 8% for the M06 family. Again, small changes are observed for TPSS. r^{2}SCAN represents an intermediate case. U^{4+} is mainly needed for stabilization and synthetic access, while the Bi_{12}^{7-} radical shell is essential for the net diatropic ring current. Only considering Bi_{12}^{7-} with the TPSS functionals leads to a nucleus-independent chemical shift[90] (NICS) of −10.9 ppm and a current strength of 14.6 nA/T. cTPSS leads to a NICS of −11.0 ppm and a current strength of 14.7 nA/T, respectively. Compared to the pNMR shieldings and the g-tensors, the impact of $\tilde{\tau}_{\mathrm{D}}$ on the ring current and the magnetically induced current density is less pronounced. Therefore, both the field-dependent and the current-dependent generalization of τ can be used to reliably study aromaticity based on the magnetic criterion.[39,91,92]

V. CONCLUSION

We have presented pNMR and EPR properties with the current-dependent generalization of the kinetic energy density. In contrast to the field-dependent generalization,[3] this restores the iso-orbital constraint[7] and removes artifacts in the paramagnetic orbital shielding contribution.[22] Substantial improvements are found for the Minnesota and SCAN functional families, while the TPSS family exhibits a moderate dependence on the generalization of τ. Compared to experimental and high-level computational references, $\tilde{\tau}_{\mathrm{D}}$ leads to more accurate results. This improvement is rather significant and strongly suggests that the generalized $\tilde{\tau}_{\mathrm{D}}$ must be employed for assessing pNMR and EPR properties of paramagnetic systems. This is especially true if no or a low amount of exact exchange is mixed in.

As an outlook, an extension of this approach to a relativistic two-component framework[61,93–95] seems promising for EPR g-tensors and hyperfine coupling constants to fully exploit the potential of meta-GGAs. Here, the paramagnetic current density in the ground state no longer vanishes and even larger changes are expected.

SUPPLEMENTARY MATERIAL

See the supplementary material for complete computational details and data.

ACKNOWLEDGMENTS

C.H. acknowledges funding from the Volkswagen Foundation. Y.J.F. acknowledges the financial support from TURBOMOLE GmbH.

AUTHOR DECLARATIONS

Conflict of Interest

The authors have no conflicts to disclose.

Author Contributions

Yannick J. Franzke: Conceptualization (equal); Data curation (equal); Formal analysis (equal); Investigation (equal); Methodology (equal); Validation (equal); Writing – original draft (equal); Writing – review & editing (equal). **Christof Holzer:** Conceptualization (equal); Formal analysis (equal); Investigation (equal); Methodology (equal); Validation (equal); Writing – original draft (equal); Writing – review & editing (equal).

DATA AVAILABILITY

The data that support the findings of this study are available within the article and its supplementary material.

REFERENCES

[1] A. D. Becke, J. Chem. Phys. **140**, 18A301 (2014).
[2] N. Mardirossian and M. Head-Gordon, Mol. Phys. **115**, 2315 (2017).
[3] S. N. Maximoff and G. E. Scuseria, Chem. Phys. Lett. **390**, 408 (2004).
[4] A. D. Becke, J. Chem. Phys. **117**, 6935 (2002).
[5] J. Tao, Phys. Rev. B **71**, 205107 (2005).
[6] M. P. Johansson and M. Swart, J. Chem. Theory Comput. **6**, 3302 (2010).
[7] J. E. Bates and F. Furche, J. Chem. Phys. **137**, 164105 (2012).
[8] K. Reiter, F. Mack, and F. Weigend, J. Chem. Theory Comput. **14**, 191 (2018).
[9] S. Lehtola, M. Dimitrova, H. Fliegl, and D. Sundholm, J. Chem. Theory Comput. **17**, 1457 (2021).
[10] S. Lehtola, M. Dimitrova, H. Fliegl, and D. Sundholm, J. Chem. Theory Comput. **17**, 4629 (2021).
[11] J. F. Dobson, J. Chem. Phys. **98**, 8870 (1993).
[12] C. Holzer, Y. J. Franzke, and M. Kehry, J. Chem. Theory Comput. **17**, 2928 (2021).
[13] Y. J. Franzke, F. Mack, and F. Weigend, J. Chem. Theory Comput. **17**, 3974 (2021).
[14] F. Bruder, Y. J. Franzke, and F. Weigend, J. Phys. Chem. A (to be published).
[15] J. Liang, X. Feng, D. Hait, and M. Head-Gordon, J. Chem. Theory Comput. **18**, 3460 (2022).

[16] E. I. Tellgren, A. M. Teale, J. W. Furness, K. K. Lange, U. Ekström, and T. Helgaker, J. Chem. Phys. **140**, 034101 (2014).

[17] J. W. Furness, J. Verbeke, E. I. Tellgren, S. Stopkowicz, U. Ekström, T. Helgaker, and A. M. Teale, J. Chem. Theory Comput. **11**, 4169 (2015).

[18] T. J. P. Irons, L. Spence, G. David, B. T. Speake, T. Helgaker, and A. M. Teale, J. Phys. Chem. A **124**, 1321 (2020).

[19] S. Sen and E. I. Tellgren, J. Chem. Theory Comput. **17**, 1480 (2021).

[20] T. J. P. Irons, G. David, and A. M. Teale, J. Chem. Theory Comput. **17**, 2166 (2021).

[21] A. Pausch and C. Holzer, J. Phys. Chem. Lett. **13**, 4335 (2022).

[22] C. J. Schattenberg and M. Kaupp, J. Chem. Theory Comput. **17**, 1469 (2021).

[23] S. Reimann, U. Ekström, S. Stopkowicz, A. M. Teale, A. Borgoo, and T. Helgaker, Phys. Chem. Chem. Phys. **17**, 18834 (2015).

[24] J. Jaramillo, G. E. Scuseria, and M. Ernzerhof, J. Chem. Phys. **118**, 1068 (2003).

[25] T. M. Maier, A. V. Arbuznikov, and M. Kaupp, Wiley Interdiscip. Rev.: Comput. Mol. Sci. **9**, e1378 (2018).

[26] E. R. Johnson, J. Chem. Phys. **141**, 124120 (2014).

[27] J. P. Perdew, V. N. Staroverov, J. Tao, and G. E. Scuseria, Phys. Rev. A **78**, 052513 (2008).

[28] V. G. Malkin, O. L. Malkina, and D. R. Salahub, Chem. Phys. Lett. **204**, 80 (1993).

[29] G. Schreckenbach and T. Ziegler, J. Chem. Phys. **99**, 606 (1995).

[30] G. Schreckenbach and T. Ziegler, J. Phys. Chem. A **101**, 3388 (1997).

[31] J. R. Cheeseman, G. W. Trucks, T. A. Keith, and M. J. Frisch, J. Chem. Phys. **104**, 5497 (1996).

[32] G. Vignale and M. Rasolt, Phys. Rev. Lett. **59**, 2360 (1987).

[33] F. London, J. Phys. Radium **8**, 397 (1937).

[34] R. Ditchfield, Mol. Phys. **27**, 789 (1974).

[35] P. Lazzeretti, Prog. Nucl. Magn. Reson. Spectrosc. **36**, 1 (2000).

[36] J. Jusélius, D. Sundholm, and J. Gauss, J. Chem. Phys. **121**, 3952 (2004).

[37] S. Taubert, D. Sundholm, and J. Jusélius, J. Chem. Phys. **134**, 054123 (2011).

[38] H. Fliegl, S. Taubert, O. Lehtonen, and D. Sundholm, Phys. Chem. Chem. Phys. **13**, 20500 (2011).

[39] D. Sundholm, H. Fliegl, and R. J. F. Berger, Wiley Interdiscip. Rev.: Comput. Mol. Sci. **6**, 639 (2016).

[40] D. Sundholm, M. Dimitrova, and R. J. F. Berger, Chem. Commun. **57**, 12362 (2021).

[41] GIMIC, Version 2.1.4 (merge 6c574ed, 2020), available from https://github.com/qmcurrents/gimic, retrieved March 28, 2021.

[42] R. J. F. Berger, M. Dimitrova, R. T. Nasibullin, R. R. Valiev, and D. Sundholm, Phys. Chem. Chem. Phys. **24**, 624 (2022).

[43] R. Ahlrichs, M. Bär, M. Häser, H. Horn, and C. Kölmel, Chem. Phys. Lett. **162**, 165 (1989).

[44] S. G. Balasubramani, G. P. Chen, S. Coriani, M. Diedenhofen, M. S. Frank, Y. J. Franzke, F. Furche, R. Grotjahn, M. E. Harding, C. Hättig, A. Hellweg, B. Helmich-Paris, C. Holzer, U. Huniar, M. Kaupp, A. Marefat Khah, S. Karbalaei Khani, T. Müller, F. Mack, B. D. Nguyen, S. M. Parker, E. Perlt, D. Rappoport, K. Reiter, S. Roy, M. Rückert, G. Schmitz, M. Sierka, E. Tapavicza, D. P. Tew, C. van Wüllen, V. K. Voora, F. Weigend, A. Wodyński, and J. M. Yu, J. Chem. Phys. **152**, 184107 (2020).

[45] Developers' version of TURBOMOLE V7.6 2021, a development of University of Karlsruhe and Forschungszentrum Karlsruhe GmbH, 1989–2007, TURBOMOLE GmbH, since 2007; available from https://www.turbomole.org, retrieved January 12, 2022.

[46] C. J. Schattenberg, K. Reiter, F. Weigend, and M. Kaupp, J. Chem. Theory Comput. **16**, 931 (2020).

[47] C. J. Schattenberg and M. Kaupp, J. Phys. Chem. A **125**, 2697 (2021).

[48] P. Plessow and F. Weigend, J. Comput. Chem. **33**, 810 (2012).

[49] H. Bahmann and M. Kaupp, J. Chem. Theory Comput. **11**, 1540 (2015).

[50] C. Holzer, J. Chem. Phys. **153**, 184115 (2020).

[51] T. H. Dunning, J. Chem. Phys. **90**, 1007 (1989).

[52] R. A. Kendall, T. H. Dunning, and R. J. Harrison, J. Chem. Phys. **96**, 6796 (1992).

[53] D. E. Woon and T. H. Dunning, J. Chem. Phys. **98**, 1358 (1993).

[54] Z. Rinkevicius, J. Vaara, L. Telyatnyk, and O. Vahtras, J. Chem. Phys. **118**, 2550 (2003).

[55] F. Weigend and R. Ahlrichs, Phys. Chem. Chem. Phys. **7**, 3297 (2005).

[56] D. Peng and M. Reiher, J. Chem. Phys. **136**, 244108 (2012).

[57] D. Peng, N. Middendorf, F. Weigend, and M. Reiher, J. Chem. Phys. **138**, 184105 (2013).

[58] Y. J. Franzke, N. Middendorf, and F. Weigend, J. Chem. Phys. **148**, 104110 (2018).

[59] Y. J. Franzke and F. Weigend, J. Chem. Theory Comput. **15**, 1028 (2019).

[60] S. Gillhuber, Y. J. Franzke, and F. Weigend, J. Phys. Chem. A **125**, 9707 (2021).

[61] Y. J. Franzke and J. M. Yu, J. Chem. Theory Comput. **18**, 2246 (2022).

[62] Y. J. Franzke, L. Spiske, P. Pollak, and F. Weigend, J. Chem. Theory Comput. **16**, 5658 (2020).

[63] N. Lichtenberger, R. J. Wilson, A. R. Eulenstein, W. Massa, R. Clérac, F. Weigend, and S. Dehnen, J. Am. Chem. Soc. **138**, 9033 (2016).

[64] X. Cao and M. Dolg, J. Mol. Struct.: THEOCHEM **673**, 203 (2004).

[65] B. Metz, H. Stoll, and M. Dolg, J. Chem. Phys. **113**, 2563 (2000).

[66] W. Küchle, M. Dolg, H. Stoll, and H. Preuss, J. Chem. Phys. **100**, 7535 (1994).

[67] F. Weigend, Phys. Chem. Chem. Phys. **8**, 1057 (2006).

[68] J. Tao, J. P. Perdew, V. N. Staroverov, and G. E. Scuseria, Phys. Rev. Lett. **91**, 146401 (2003).

[69] V. N. Staroverov, G. E. Scuseria, J. Tao, and J. P. Perdew, J. Chem. Phys. **119**, 12129 (2003).

[70] J. W. Furness, A. D. Kaplan, J. Ning, J. P. Perdew, and J. Sun, J. Phys. Chem. Lett. **11**, 8208 (2020).

[71] J. W. Furness, A. D. Kaplan, J. Ning, J. P. Perdew, and J. Sun, J. Phys. Chem. Lett. **11**, 9248 (2020).

[72] M. Bursch, H. Neugebauer, S. Ehlert, and S. Grimme, J. Chem. Phys. **156**, 134105 (2022).

[73] J. Tao and Y. Mo, Phys. Rev. Lett. **117**, 073001 (2016).

[74] Y. Zhao and D. G. Truhlar, J. Chem. Phys. **125**, 194101 (2006).

[75] Y. Zhao and D. G. Truhlar, Theor. Chem. Acc. **120**, 215 (2008).

[76] R. Peverati and D. G. Truhlar, J. Phys. Chem. Lett. **3**, 117 (2012).

[77] R. Peverati and D. G. Truhlar, J. Phys. Chem. Lett. **2**, 2810 (2011).

[78] R. Peverati and D. G. Truhlar, Phys. Chem. Chem. Phys. **14**, 13171 (2012).

[79] R. Peverati and D. G. Truhlar, Phys. Chem. Chem. Phys. **14**, 16187 (2012).

[80] H. S. Yu, X. He, and D. G. Truhlar, J. Chem. Theory Comput. **12**, 1280 (2016).

[81] H. S. Yu, X. He, S. L. Li, and D. G. Truhlar, Chem. Sci. **7**, 5032 (2016).

[82] J. P. Perdew, S. Kurth, A. Zupan, and P. Blaha, Phys. Rev. Lett. **82**, 2544 (1999).

[83] A. D. Boese and J. M. L. Martin, J. Chem. Phys. **121**, 3405 (2004).

[84] N. Mardirossian and M. Head-Gordon, J. Chem. Phys. **142**, 074111 (2015).

[85] N. Mardirossian and M. Head-Gordon, J. Chem. Phys. **144**, 214110 (2016).

[86] T. Aschebrock and S. Kümmel, Phys. Rev. Res. **1**, 033082 (2019).

[87] A. V. Arbuznikov and M. Kaupp, J. Chem. Phys. **136**, 014111 (2012).

[88] M. Haasler, T. M. Maier, R. Grotjahn, S. Gückel, A. V. Arbuznikov, and M. Kaupp, J. Chem. Theory Comput. **16**, 5645 (2020).

[89] A. R. Eulenstein, Y. J. Franzke, N. Lichtenberger, R. J. Wilson, H. L. Deubner, F. Kraus, R. Clérac, F. Weigend, and S. Dehnen, Nat. Chem. **13**, 149 (2021).

[90] P. von Ragué Schleyer, C. Maerker, A. Dransfeld, H. Jiao, and N. J. R. van Eikema Hommes, J. Am. Chem. Soc. **118**, 6317 (1996).

[91] P. R. von Schleyer and H. Jiao, Pure Appl. Chem. **68**, 209 (1996).

[92] R. Gershoni-Poranne and A. Stanger, Chem. Soc. Rev. **44**, 6597 (2015).

[93] Y. J. Franzke and J. M. Yu, J. Chem. Theory Comput. **18**, 323 (2022).

[94] A. Wodyński and M. Kaupp, J. Chem. Theory Comput. **16**, 314 (2020).

[95] C. Holzer and Y. J. Franzke, J. Chem. Phys. (published online, 2022).